J|A|C|S COMMUNICATIONS

Published on Web 12/30/2008

Intercalation of Aggregation-Free and Well-Dispersed Gold Nanoparticles into the Walls of Mesoporous Silica as a Robust "Green" Catalyst for *n*-Alkane Oxidation

Lifang Chen,[†] Juncheng Hu,*[,‡] and Ryan Richards*[,†]

Department of Chemistry and Geochemistry, Colorado School of Mines, Golden, Colorado 80401, and Key Laboratory of Catalysis and Materials Science of the State Ethnic Affairs Commission & Ministry of Education, South-Central University for Nationalities, Wuhan, 430074, P.R. China

Received November 11, 2008; E-mail: jchuhu@yahoo.com; rrichard@mines.edu

In recent years, catalysis by gold has become one of the most intensively studied topics in chemistry.[1,2] Au-based catalysts have demonstrated very promising activity and selectivity in many chemical processes, and generally, the catalytic properties of heterogeneous Au catalysts have been found to strongly depend on the particle size and stability. The use of Au as a catalyst requires careful and often unconventional preparation of the Au metal, focused on achieving very small and stable Au particles (<5 nm). Au nanoparticles (NPs) are however mobile on the surface of most supporting oxides, and at present, one of the key problematic issues impeding the application of Au catalysts is the stability of the particles against sintering under reaction conditions.[3]

The selective oxidation of hydrocarbons, the targeted addition of oxygen atoms to produce specific desired reaction products, is crucial in industrial petroleum-based chemical processes.[4] The ideal "green" catalyst would use air as the oxidant under mild conditions, be recyclable, and would avoid the wasteful addition of reducing agents and solvents. Many challenges are associated with the realization of these goals due to difficulties associated with oxygen and substrate activation and the fact that the solvent plays an important role in the activity of the catalysts for the oxidation of alkanes.[5] Some catalysts have been used for cycloalkane oxidation successfully;[6,7] however for *n*-alkanes, only a few catalytic systems have been reported, and most are in combination with additives such as reducing agents and radical initiators in solvents or under severe conditions.[8−10] We have previously reported Au NPs confined in the walls of mesoporous silica for aerobic oxidation of alcohols; however, these catalysts showed irregular shapes and pores.[11] Here, we present an improved method to synthesize a supported robust nanogold "green" catalyst. For the catalyst, the morphology and pore order can be controlled; the aggregate-free Au NPs are highly dispersed and intercalated into the walls of mesoporous silica and showed high catalytic activity in the oxidation of *n*-alkane.

The well-dispersed Au NPs were successfully intercalated into the walls of mesoporous silica by a simple technique, which has been described in detail in the Supporting Information. According to the different Au weight percents and 1,4-bis(triethoxysily)propane tetrasulfide (TESPTS) in the mesoporous silica and morphology, these materials were referred to as 2-10-GMS (Au in mesoporous silica) and 2-2-GMS. When 10% of TESPTS was added, the 2-10-GMS shows irregular shapes and wormhole-like pores (Figure S1a and b). When the ratio of TESPTS/TEOS was decreased to 2%, ordered mesoporous nanocomposites were obtained, referred to as 2-2-GMS. Figure 1A shows the scanning electron microscopy (SEM) images of 2-2-GMS, appearing as a whorl with a diameter of ∼200 nm and a length of 2 μm. Figure 1B and 1C, respectively, show high resolution transmission electron microscopy (HRTEM) images of a hexagonal mesoporous 2-2-GMS along the (100) and (110) planes and clearly demonstrate the mesoporous structure. The red arrows point out the Au particles distribution within the matrix; thus here we can observe that all of the Au particles synthesized by this pathway are well-dispersed and intercalated in the walls of the mesoporous silica. The size distribution of these particles reveals an average particle diameter of ∼2 nm. Moreover, with a wall thickness of 4−8 nm, the materials are unusually stable to high temperature. Because the NPs are well segregated and protected by walls, sintering upon calcination at elevated temperature is limited.[12−15] The broadened XRD peaks of Au (111) and (200) in Figure 1D indicate that the Au particles are nanoscale. Figure S2 shows a UV−vis absorption spectrum of the 2-2-GMS with a band centered at 509 nm indicating an average particle diameter of less than 5 nm. The 2-2-GMS materials have similar nitrogen sorption isotherms to SBA-15 with very narrow pore-size distributions centered at ∼5.6 nm shown in Figure S3a, which are typical for mesoporous materials. The surface area of 2-2-GMS is 800 $m^2 \cdot g^{-1}$ with a pore size of 5.6 nm. Figure S4 presents the DRIFTS spectra of the 2-2-GMS catalyst before and after calcination. After calcination, the characteristic peaks between 2800 and 3000 cm^{-1} are not observed, inferring that the organic components are removed completely during the calcination.

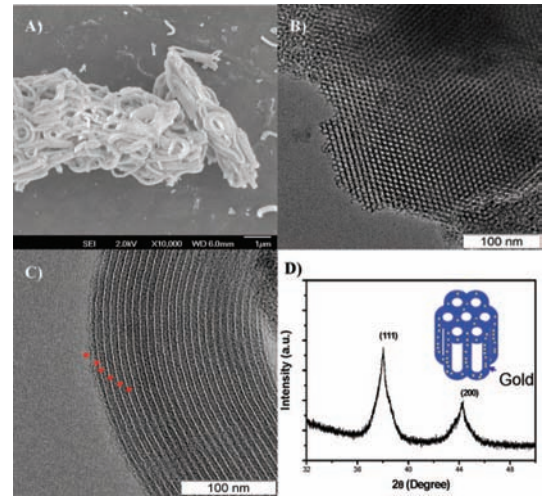

Figure 1. (A) SEM image of 2-2-GMS; (B and C) HRTEM images of 2-2-GMS, (D) XRD pattern of 2-2-GMS; the inset is a model of 2-2-GMS.

[†] Colorado School of Mines.
[‡] South-Central University for Nationalities.

10.1021/ja808860v CCC: $40.75

Table 1. Results of *n*-Hexadecane Oxidation to Ketones and Alcohols[a]

catalyst	BET surface area (m^2/g)	n-$C_{16}H_{34}$ conv. (mol %)[b]	product selectivity[c] (mol%) and distribution			
			ketones[d]	TOF (1/h)[e]	alcohols[f]	TOF (1/h)[g]
2-2-GMS	800	52.3	46 (11:31:9:10:15:16:8)	892	25 (36:10:12:18:11:13)	485
Au-SH-SBA-15	194	27.8	48 (15:25:10:10:15:15:10)	218	27 (26:9:11:17:16:21)	123
2-Au-SBA-15	240	17.6	47 (14:26:8:7:12:18:15)	306	30 (31:11:8:16:22:6:6)	196
2-TESPTS-SBA-15	950	7.0	49 (16:27:9:9:11:18:10)	–	29 (30:10:18:16:11:13)	–
2-2-GMS (2nd use)	–	50.6	47 (15:27:9:9:15:17:8)	881	24 (28:9:10:19:16:18)	450
2-2-GMS (3rd use)	–	47.1	47 (16:28:9:9:14:14:10)	820	28 (29:9:12:18:15:17)	489

[a] Reaction conditions: 10 mg catalyst, 5 mL of *n*-hexadecane, airflow rate 30 mL/min, temperature 150 °C, reaction time 6 h. [b] *n*-Hexadecane conv. (%) = reacted *n*-hexadecane/introduced *n*-hexadecane. [c] Product selectivity: ketones or alcohols (%) = produced ketones or alcohols/reacted *n*-hexadecane. [d] Values in parentheses represent 7-, 6-, 5-, 4-, 3-, 2-, and 1-hexadecanone, respectively. [e] Moles of ketones produced per moles of Au per hour. [f] Values in parentheses represent 7-, 6-, 5-, 4-, 3-, and 2-hexadecanol, respectively. [g] Moles of alcohols produced per moles of Au per hour.

The oxidation of *n*-alkanes is an important reaction for the conversion of saturated hydrocarbons to their corresponding alcohols and ketones. The use of Pd metal and Pd organic complexes for *n*-alkane oxidation is well-known.[16,17] In the present work, we found that Au NPs intercalated in mesoporous silica are exceptionally good catalysts for solvent-free aerobic oxidation of *n*-hexadecane. The catalytic results are summarized in Table 1. For the 2-2-GMS catalyst, a conversion of 52.3% was obtained and the total selectivity to ketones and alcohols was 71%; it is noteworthy that the turnover frequencies were very high.

For comparison, the catalytic activities of thiol group modified SBA-15 anchored Au (Au-SH-SBA-15, Figure S5) in the pores of mesoporous silica and 2-Au-SBA-15 were also investigated and demonstrate conversions of *n*-hexadecane of 27.8% and 17.6%, and the selectivities to ketones and alcohols were 75% and 77%, respectively. The 7% conversion of *n*-hexadecane in the presence of 2-TESPTS-SBA-15 is likely due to auto-oxidation. The conversion of *n*-hexadecane over the 2-2-GMS catalyst was nearly twice that of Au-SH-SBA-15 (4 wt% Au) although the Au loading was lower. Au catalyst performance often depends on the site density, size, stability, the oxidation state of Au NPs, support interaction, and Au capture efficiency of the support.[18−20] In our case, for the Au-SH-SBA-15 and the 2-Au-SBA-15 catalysts, the Au NPs are located in the main channels and the particle diameters are similar to the channels (5−8 nm); these particles block the main channels, and most of those particles in the middle of the channels are not readily accessible during the reaction. This is supported by the decrease of surface area from 800 to 194 m^2/g in Table 1. While the Au NPs of 2-2-GMS are in the walls, the high activity may be due to the unobstructed mesoporous structure of 2-2-GMS, the particles close in proximity to the mesopore surface providing enhanced accessibility and/or the smaller size (ca. 2 nm) of the Au NPs. The sizes of these particles in different samples are confirmed by the full width at half-height (fwhh) of the XRD patterns as shown in Figure S7. Moreover, Figure S6 is a TEM image of the 2-2-GMS catalyst after reaction demonstrating the Au NPs were still intercalated in the walls of mesoporous silica and indicating that sintering of Au NPs had not taken place. The stability of the 2-2-GMS can be confirmed by the XRD patterns before and after catalytic reaction as shown in Figure S8. The unique structure of the 2-2-GMS catalyst demonstrates it can be conceptualized as a nanoreactor with many advantages. First, each NP is isolated by the walls with the ordered and stable mesoporous wall structure also hindering the aggregation of neighboring particles, even under relatively harsh reaction conditions. Second, the mesoporous channels offer a large surface area, desirable for mass and heat transfer, feasibly leading to high catalytic activity. The conversion of *n*-hexadecane only decreased from 52.3% to 47.1% for the third use, indicating the 2-2-GMS could be stable and recycled. The activity decrease may be due to the adsorption of some reactant or products on the surface of the catalyst after recycling.

In summary, we have successfully demonstrated the synthesis of stable nanogold/mesoporous silica composites with significantly improved catalytic activity for *n*-hexadecane oxidation. We believe that the ordered mesoporous structure without blocking of 2-2-GMS catalyst and the small size of Au NPs are the main factors leading to the high catalytic activity. The catalyst systems are chemically and mechanically robust, can be separated easily, and are reusable, demonstrating attractive potential for practical applications. This work also provides a new pathway to design and fabricate stable mesoporous materials containing metal nanoparticles for catalysis and other applications.

Acknowledgment. Ryan Richards and Lifang Chen thank Colorado School of Mines for research support. This work was supported by NSFC (20803096) and South-Central University for Nationalities (YZZ08002).

Supporting Information Available: Detailed preparation, characterization (XRD, SEM, TEM, N_2 adsorption, and DRIFTS) and catalytic tests of these nanocomposites. This material is available free of charge via the Internet at http://pubs.acs.org.

References

(1) Enache, D. I.; Knight, D. W.; Hutchings, G. J. *Catal. Lett.* **2005**, *103*, 43.
(2) Abad, A.; Concepcion, P.; Corma, A.; Garcia, H. *Angew. Chem., Int. Ed.* **2005**, *44*, 4066.
(3) Corti, C. W.; Holliday, R. J.; Thompson, D. T. *Appl. Catal. A: General* **2005**, *291*, 253.
(4) Haruta, M. *Nature* **2005**, *437*, 1098.
(5) Vincent, J. M.; Rabion, A.; Yachandra, V. K.; Fish, R. H. *Angew. Chem., Int. Ed. Engl,* **1997**, *36*, 2346.
(6) Solsona, B. E.; Garcia, T.; Jones, C.; Taylor, S. H.; Carley, A. F.; Hutchings, G. J. *Appl. Catal. A: General* **2006**, *312*, 67.
(7) Hughes, M. D.; Xu, Y. J.; Jenkins, P.; McMorn, P.; Landon, P.; Enache, D. I.; Carley, A. F.; Attard, G. A.; Hutchings, G. J.; King, F. K.; Stitt, E. H.; Johnston, P.; Griffin, K.; Kiely, C. J. *Nature* **2005**, *437*, 1132.
(8) Neumann, R.; Dahan, M. *Nature* **1997**, *388*, 353.
(9) Shinachi, S.; Matsushita, M.; Yamaguchi, K.; Mizuno, N. *J. Catal.* **2005**, *233*, 81.
(10) Hayashi, T.; Kishida, A.; Mizuno, N. *Chem. Commun.* **2000**, 381.
(11) Hu, J.; Chen, L.; Zhu, K.; Suchopar, A.; Richards, R. *Catal. Today* **2007**, *122*, 277.
(12) Arnal, P. M.; Comatti, M.; Schüth, F. *Angew. Chem., Int. Ed.* **2006**, *45*, 8224.
(13) Garcia, C.; Zhang, Y.; DiSalvo, F.; Wiesner, U. *Angew. Chem., Int. Ed.* **2003**, *42*, 1526.
(14) Yang, C.; Lin, H.; Zibrowius, B.; Spliethoff, B.; Schüth, F.; Liou, S.; Chu, M.; Chen, C. *Chem. Mater.* **2007**, *19*, 3205.
(15) Yuranov, I.; Kiwi-Minsker, L.; Buffat, P.; Renken, A. *Chem. Mater.* **2004**, *16*, 760.
(16) Lin, M.; Sen, A. J. *J. Am. Chem. Soc.* **1992**, *114*, 7307.
(17) Sen, A.; Gretz, E.; Oliver, T. F.; Jiang, Z. *New J. Chem.* **1989**, *13*, 755.
(18) Sacaliuc-Parvulescu, E.; Friedrich, H.; Palkovits, R.; Weckhuysen, B. M.; Nijhuis, T. A. *J. Catal.* **2008**, *259*, 43.
(19) Sacaliuc, E.; Beale, A. M.; Weckhuysen, B. M.; Nijhuis, T. A. *J. Catal.* **2007**, *248*, 235.
(20) Cumaranatunge, L.; Delgass, W. N. *J. Catal.* **2005**, *232*, 38.

JA808860V